Solvation pressure in ethanol by molecular dynamics simulations

Peter J. Berryman and David A. Faux*
Advanced Technology Institute, University of Surrey, Guildford GU2 4ES, United Kingdom

David J. Dunstan
Department of Physics, Queen Mary, University of London, London E1 4NS, United Kingdom
(Received 1 February 2007; revised manuscript received 23 April 2007; published 12 September 2007)

The results of all-atom molecular dynamics simulations of ethanol liquid and vapor using a modified version of the Cornell field [W. D. Cornell and P. Cieplak, J. Am. Chem. Soc. **117**, 5179 (1995)] are presented. Excellent agreement with experiment is obtained for density, compressibility, and cohesive energy density. The ethanol liquid is subjected to uniform hydrostatic pressure in the range −1 to 15 kbar at room temperature and the vibrational frequency spectra are calculated. The peak frequencies of seven major vibrational modes are found to be accurate to within 100 cm^{-1} of their experimental positions and the change of frequency as a function of pressure is consistent with Raman data. The change in bond length is found to be consistent with the solvation pressure model for all bonds except for O-H due to hydrogen bonding.

DOI: 10.1103/PhysRevB.76.104303 PACS number(s): 78.30.Cp, 62.50.+p, 31.70.Dk, 33.20.Fb

I. INTRODUCTION

There is a considerable interest at the interface of physics, chemistry, and biology, on the response of solvated molecules to the physical environment, and the behavior of molecules and nanoparticles immersed in a liquid can be complex. It is apparent that the solvent that surrounds a molecule may have an important *physical* effect on the molecule. The solvent exerts a pressure, called *solvation pressure*, which acts in addition to any externally applied pressure. In general, one of the effects of the solvation pressure is to compress molecular bonds. The shortening of molecular bonds leads to an associated increase in bond vibrational frequencies which can be measured using Raman spectroscopy. The solvation pressure effect has been observed using Raman spectroscopy for nanosized objects such as carbon nanotubes,[1–3] starch grains,[4] and for solvent mixtures.[5,6]

The folding of proteins is an important example of how a molecule responds to its physical environment and life depends on the ability of proteins in an aqueous environment to switch reversibly between complex folded structures and various degrees of unfolding. The consequences of incorrect folding are seen in the prion diseases, scrapie in sheep, BSE in cattle, and new-variant C Jakob disease and Alzheimer's disease in humans. Proteins may reconfigure in response to *p*H and ion concentration, as well as to the thermodynamic variables of temperature and pressure.[7,8] Hydrogen bonding is also known to influence protein folding.[9]

In this paper, we examine the solvation pressure effect on ethanol, a hydrogen-bonded liquid. One of the aims of this work is to establish the limitations of the solvation pressure model for ethanol. Ethanol is chosen for two reasons: first, excellent experimental data are available for bulk properties and for the Raman spectra as a function of applied pressure; second, ethanol contains many of the bond types found in proteins and so can serve as a relatively simple prototype to a protein system.

The solvation pressure model states that the pressure experienced by the solute is equal to the cohesive energy density (CED) of the solvent, defined as the energy of vaporization per unit volume,

$$\mathrm{CED} = \frac{\Delta U_{vap}}{V_L}, \tag{1}$$

where ΔU_{vap} is the molar internal energy change on vaporization and V_L is the molar volume of the liquid. The internal energy change on vaporization is easily obtained from a molecular dynamics simulation but, experimentally, it is ΔH_{vap}, the molar enthalpy of vaporization, that is measured. The two molar energies are related by

$$H_{vap} = U_{vap} + PV_{vap}, \tag{2}$$

where V_{vap} is the molar volume of the vapor and P is the pressure. A similar expression can be written for the liquid phase and since $V_{vap} \gg V_L$, it is straightforward to show that

$$\Delta H_{vap} = \Delta U_{vap} + RT, \tag{3}$$

assuming that the van der Waals formula holds for the vapor. Thus, the CED can be deduced from a measurement of the molar enthalpy of vaporization through Eqs. (1) and (3) and is often expressed in pressure units. For example, the CED of water is about 24 kbar, about 7 kbar for ethanol, and 3 kbar for chloroform ($1\ \mathrm{J\ m^{-3}} \equiv 10^{-5}$ bar). It is immediately evident that there is the prospect of using solvent mixtures, in principle, to control the effective pressure experienced by nanosized objects contained in the mixture.[10]

It is noted that the internal pressure of a liquid, π_{int}, is defined as the derivative of its internal energy with respect to volume so that

$$\pi_{int} = \left(\frac{\partial U}{\partial V}\right)_T = n\frac{\Delta U_{vap}}{V_L}, \tag{4}$$

where n is a dimensionless ratio which has been related to the strength of the intermolecular forces in the liquid[11] and may also indicate the likely validity of the solvation pressure model. For example, $n \approx 1$ for nonpolar liquids and $n \approx 0.43$ for ethanol.[12]

 ©2007 The American Physical Society

The solvation pressure or an applied external uniform hydrostatic pressure will tend to reduce the mean bond lengths in a solute molecule. A molecule immersed in a solvent with a high CED should reveal bond lengths that would be, on average, shorter for the same molecule in a solvent with a low CED. Direct measurements of these bond lengths are difficult to obtain but can be deduced from Raman spectroscopy. Here, the vibrational frequencies of the various modes of vibration of a molecule are obtained and, by performing experiments under uniform hydrostatic pressure, the change in frequency with applied pressure for key modes can be obtained. In general, as the applied pressure is increased, the bond lengths become shorter and the frequencies tend to increase. The equivalence of an applied external hydrostatic pressure and solvation pressure can be tested by comparing the change in the vibrational frequency of a particular bond type to the vapor molecule. The change in the vibrational frequency of a molecule of ethanol vapor when immersed in ethanol liquid, for example, should be equivalent to about 7 kbar of hydrostatic pressure applied to the liquid if the solvation pressure is a real pressure experienced by each molecule.

There are also, of course, many alternative theoretical models to describe how solute molecules are affected by solvent-solute interactions, notably, the statistical mechanical theory invoking competition between short-range (hard sphere) and long-range solvent-solute interactions of Schweizer and Chandler.[13] This theory has been developed further by many authors.[14,15] Good agreement with experiment has often been found but with sensitive dependence on fitting parameters such as the hard-sphere radius of the solvent and the length scales of attractive solvent-solute interactions.[15]

The strength of the solvation pressure model is its simplicity. The pressure effect of a solvent on a solute can be obtained simply from the CED of the liquid. However, the extent of the applicability of the solvation pressure model is not well known and it is not expected that the solvation pressure will always be the dominant physical effect. For example, a high degree of local order or complex interatomic interactions, such as hydrogen bonding, might lead to interactions that dominate and hence mask the ubiquitous solvation pressure effect.

This paper reports the results of extensive explicit-atom molecular dynamics simulations of pure ethanol liquid and vapor. Here, ethanol acts as both the solvent and solute. We show that the change in bond length with pressure is well described by the solvation pressure model for all bonds except for O-H due to masking by hydrogen-bonding forces.

II. MOLECULAR DYNAMICS SIMULATIONS

A. Ethanol model

Atom-specific potentials are required for the simulation of ethanol liquid as one of the aims is to examine the vibrational properties of specific bonds. Cornell potentials for organic molecules[16] were chosen as they are atom specific, functional forms are simple, the bulk properties of ethanol at room temperature are well reproduced, and simulations are more stable than the Dreiding[17] potentials used in the previous work.[4]

TABLE I. The parameters used with Eq. (5) to define two-body intra-atomic potentials. The parameters for the C-H bond are described in text.

Bond type	k (kcal mol^{-1} Å^{-2})	r_0 (Å)
C-C	400.0	1.526
C–O	400.0	1.410
O-H	600.0	0.960

In the Cornell model, all intramolecular bonds are simple harmonic potentials given by

$$U(r) = \frac{1}{2}k(r - r_0)^2, \tag{5}$$

where k is the spring constant, r is the distance between the bonded atoms, and r_0 is the equilibrium distance between bonded atoms. Three-body angular potentials are also harmonic,

$$U(r) = \frac{1}{2}k(\theta - \theta_0)^2, \tag{6}$$

where θ is the angle formed by two bonds and θ_0 is the equilibrium angle. Finally, the dihedral four-body potentials are of the form

$$U(r) = A[1 + \cos(m\phi - \delta)], \tag{7}$$

where ϕ is the dihedral angle.

During the initial testing of this model, it was found necessary to replace the simple harmonic term describing the C-H bonds with a more accurate Morse potential in order to reproduce the high frequency carbon-hydrogen vibrational modes. The Morse potential is defined as

$$U(r) = E_0(\{1 - \exp[-k(r - r_0)]\}^2 - 1), \tag{8}$$

with values given as in the Dreiding model, namely, $E_0 = 70$ kg m^2 s^{-2}, $r_0 = 1.09$ Å, and $k = 2.24$ Å^{-1}.

Intermolecular forces are modeled with Lennard-Jones (12-6) potentials,

$$U(r) = \left(\frac{A}{r^{12}}\right) - \left(\frac{B}{r^6}\right), \tag{9}$$

and Coulombic two-body terms, whose charges are given by the restrained electrostatic potential (RESP) model[18] as provided by Cheatham *et al.*[19] All parameters are presented in Tables I–V.

B. Simulation of ethanol liquid and vapor

All molecular dynamics (MD) simulations were undertaken using the DLPOLY package.[22] The ethanol liquid consisted of a cube containing 100 ethanol molecules initially

TABLE II. The parameters used with Eq. (6) to define three-body intra-atomic potentials.

Angle type	k (kcal mol^{-1} rad^{-2})	θ_0 (deg)
HĈH	70.0	109.5
HĈC	100.0	109.5
CĈH	70.0	109.5
CÔH	110.0	108.5
HĈO	100.0	109.5

placed at random in a volume approximately 10% larger than the expected volume for the experimental density of liquid ethanol. Periodic boundary conditions were employed in the normal way. The system energy was minimized for approximately 10^6 time steps of 0.2 fs within the *NVE* ensemble (constant number of particles, volume, and energy). The temperature was then raised in 50 K steps to 298 K as an *NVT* ensemble (constant number of particles, volume and temperature) using the Nosé-Hoover thermostat and equilibrated for about 10^6 time steps at each stage. Finally, the volume was reduced using a *NPT* ensemble (constant number of particles, pressure, and temperature) using a short time step of 0.0002 fs with a target pressure of 30 kbar. The target pressure is not reached during the short *NPT* run but the cell dimension reduces by about 0.01 nm. Equilibration for about 10^6 time steps of 0.2 fs is followed by a repeat of the *NPT* run to reduce the volume further. Repetition of this *NVT-NPT* sequence produces a simulation cell containing 100 ethanol molecules at normal temperature and pressure. Further repetitions of the *NVT-NPT* cycle produce simulation cells containing ethanol prepared at a range of pressure from about −1 to 15 kbar.

MD simulations were then undertaken using the *NVE* ensemble for 10^6 time steps of 0.2 fs with the thermodynamic data recorded every 100 time steps and the atomic positions every 25 time steps. It is noted that use of the *NVE* ensemble at this stage is essential as the normal thermostat (Nosé-Hoover) for *NVT* ensembles scales the atomic velocities and the normal barostat (Berendsen) for *NPT* ensembles scales the volume and hence bond lengths. Both therefore interfere with quantities we wish to measure. The pressure was monitored throughout each run and equilibrium was verified by ensuring that there was no pressure drift. The standard deviation of the pressure fluctuations was typically 1.5 kbar.

TABLE III. The parameters used with Eq. (7) to define the dihedral intra-atomic potentials.

Dihedral	A (kcal mol^{-1})	δ (deg)	m
HCCH	0.16	0.00	3.00
HCCO	0.16	0.00	3.00
CCOH	0.17	0.00	3.00
HCOH	0.17	0.00	3.00

TABLE IV. The van der Waals parameters defining the interactions between atoms in different molecules. H_3 refers to the three hydrogen atoms attached to the carbon atom at the head of the molecule, H_2 refers to the two hydrogen molecules attached to the central carbon atom, and H_O refers to the hydrogen atom bonded to the oxygen.

Lennard-Jones pair	A (kcal Å^{12} mol^{-1})	B (kcal Å^6 mol^{-1})
C-H_2	2.29×10^4	105
C-C	1.04×10^6	676
C-H_C	0.0	0.0
C-O	7.91×10^5	693
C-H_3	9.61×10^4	126
H_2-O	4.63×10^4	103
H_3-O	6.77×10^4	124
O-O	5.82×10^5	700
H_2-H_2	3260	14.3
H_3-H_3	7520	21.7
H_2-H_3	4990	17.7
O-H_O	0.0	0.0
H_O-H_O	0.0	0.0
H_2-H_O	0.0	0.0
H_3-H_O	0.0	0.0

The vibrational frequency spectrum was obtained from the atomic velocities by evaluating the velocity autocorrelation function, namely,

$$R_v(t) \equiv \lim_{T\to\infty} \frac{1}{T}\int_0^T v(\tau)v(t+\tau)d\tau, \tag{10}$$

where $v(t)$ is the velocity of an atom at time t with averaging over all atoms in all molecules and all possible time origins. The Fourier transform of $R_v(t)$ yields the vibrational spectrum. In this case, due to the duration and time between data acquisition, data were in the range 0–3300 cm^{-1} at a resolution of 3.33 cm^{-1}. The resolution is comparable to the experimental data and was limited by the amount of velocity data that could be stored prior to processing.

The choice of system size (100 molecules, 900 atoms) was constrained by the need for lengthy simulations for statistical averaging and the need to record the atomic positions

TABLE V. The charges from the RESP model for ethanol (Ref. 19) Here, C_2 refers to the central carbon atom.

Atom type	Charge
C_1	−0.0990
H_3	0.0345
C_2	0.3318
H_2	−0.0294
O	−0.6718
H	0.4143

TABLE VI. Some bulk properties of ethanol from simulation and experiment (Ref. 23).

Property	Simulation	Expt.
Density (kg m^{-3})	810±0.01	789
Compressibility (GPa^{-1})	1.14±0.05	1.12
Cohesive energy density (kbar)	6.52±0.01	6.76

and velocities at very short time intervals in order to achieve good resolution in the vibrational spectra, producing very large output data sets. Larger simulations were not practical and, while the possibility of finite-size effects cannot be excluded, we believe that simulations of 900 atoms are large enough for these effects to be small. For example, Allen and Tildesley note that simulations of several hundred atoms are sufficient for finite-size effects to be negligible[20] and Heyes *et al.*[21] observe for a variety of physical quantities that finite-size effects are negligible for hard-sphere fluids in simulations in excess of about 1000 particles.

III. RESULTS AND DISCUSSION

Table VI shows some bulk properties of ethanol determined from the simulation. The cohesive energy density was calculated using Eq. (1), where the internal energy change on vaporization was obtained by subtracting the internal energy of the vapor from the average internal energy for the liquid under zero pressure.

The CED was calculated to be 6.52 kbar which is in very good agreement with the experimental value of 6.76 kbar. The density was found to be in good agreement with experiment, showing a 2.6% deviation from the experimental value. The compressibility C was calculated using

$$C = \frac{1}{V}\left.\frac{\partial V}{\partial P}\right|_{P=0}. \tag{11}$$

The volume per mole was plotted against the volume at zero pressure and the gradient was divided by the intercept to give a value for the compressibility, which was consistent with experiment within experimental error.

Figure 1 shows the C-H_3, C-H_2, and C-C bond lengths of ethanol as a function of pressure. The bond lengths for the vapor are plotted at −6.76 kbar, equal to the CED of the liquid, as the vapor will not experience the solvation pressure felt by the liquid. The line is obtained from the linear regression of the liquid-only data. The error bars on the vapor data represent a standard error of 10^3 separate vapor data runs. The line passes through the vapor data in each case, within error, consistent with the solvation pressure model. In other words, the application of a uniform hydrostatic pressure compresses the C-H_3, C-H_2, and C-C bond lengths in the same manner as the solvation pressure acting on the liquid at normal pressure compared to the vapor.

Figure 2 shows the length of the C-O and O-H bonds, again as a function of pressure. The O-H bond increases in length as a function of applied pressure and neither bond appears to give a fit to the solvation pressure model, a fact

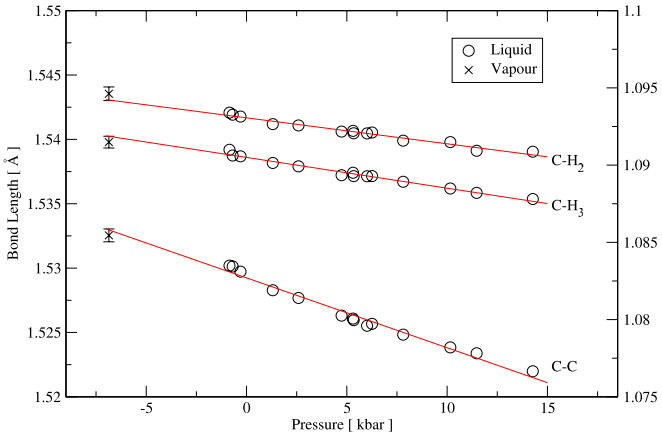

FIG. 1. (Color online) The bond lengths of C-H_3, C-H_2 (right scale), and C–C (left scale) in ethanol determined from molecular dynamics simulation as a function of uniform hydrostatic pressure. The ethanol vapor data are offset by the pressure equivalent of the cohesive energy density.

which can be attributed to the strength of the hydrogen bonding on the O-H tail, as will be discussed later.

The simulated vibrational spectra were obtained by computing the autocorrelation function and Fourier transforming, as described in the previous section. The peaks were then fit to a Lorentzian to determine the peak position. In order to assist with the identification of modes, it was possible to compute the autocorrelation function using only atoms of interest, for example, to place the C-C-O modes, one can perform the Fourier transform using only those atoms. Seven clear modes are the C-C-O symmetric stretch, C-C-O antisymmetric stretch, C-H_3 rock + C-O stretch + in plane C-O-H deformation, CH_2 twist and in-plane C-O-H deformation, C-H_3 deformation, C-H_2 symmetric stretch, and C-H_3 stretch (Table VII). Figure 3 shows a typical spectrum obtained from the simulation and compared to the Raman spectrum from experiment.[4]

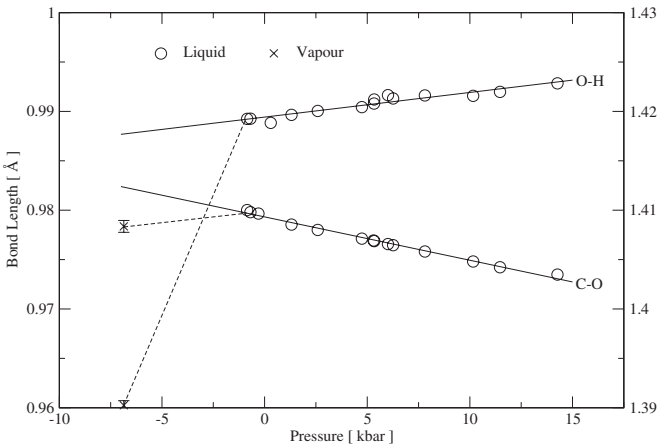

FIG. 2. The bond lengths of C-O (right scale) and O–H (left scale) in ethanol determined from molecular dynamics simulation as a function of uniform hydrostatic pressure. The ethanol vapor data are offset by the pressure equivalent of the cohesive energy density.

TABLE VII. The peak position of major vibrational modes of ethanol compared with the Raman spectrum from experiment (Ref. 4).

Label	Raman mode	Peak position MD (cm^{-1})	Peak position Expt. (cm^{-1})
CCOs	CCO symmetric stretch	815	883
CCOa	CCO antisymmetric stretch	1082	1051
MO_2	CO stretch+CH_3 rock+in plane COH deformation	1173	1096
MO_1	CH_2 twist+in plane COH deformation	1296	1276
CH_3d	CH_3 deformation	1420	1453
CH_2	CH_2 symmetric stretch	2896	2881
CH_3s	CH_3 stretch	2948	2928

The peak position of some vibrational modes of ethanol as a function of applied uniform hydrostatic pressure are shown in Fig. 4, with the vapor data again representing the average of 10^3 separate vapor simulations. Despite the large number of vapor simulations performed, the resulting vibrational spectrum is subject to significant statistical fluctuations because there is only one bond to analyze per time step. The errors on the vapor data are larger than for the bond lengths due to the uncertainty in fitting a Lorentzian to peaks which are subject to statistical variation. However, the errors of around ± 3 cm^{-1} are not large enough to distract from the general trends in data. The straight lines are guides to the eyes and represent linear regression of the liquid data only. In Fig. 4, all modes increase in frequency from vapor to liquid consistent with the solvation pressure model for these modes in ethanol.

The CH_2 twist and in plane C-O-H deformation mode MO_1 (Fig. 5) appear to split in the vapor phase, producing two distinct peaks in the vapor vibrational spectra where only a single combined peak appeared in the liquid phase. The average of these two peaks gives a point which is consistent with the solvation pressure model. It would appear that the C-O-H deformation mode occurs at a higher frequency in the vapor phase than in the liquid. This is consistent with the bond length data which shows the O-H bond to be stretched by hydrogen bonding in the liquid phase. The anomalous behavior of a hydrogen-bonding group in the Raman peak has been observed on many occasions (for example, Ref. 14) since first noted by Drickamer and co-workers[24,25] on butanol. In ethanol, too, the strength of the hydrogen bonding dominates over the van der Waals interaction responsible for the solvation pressure effect.

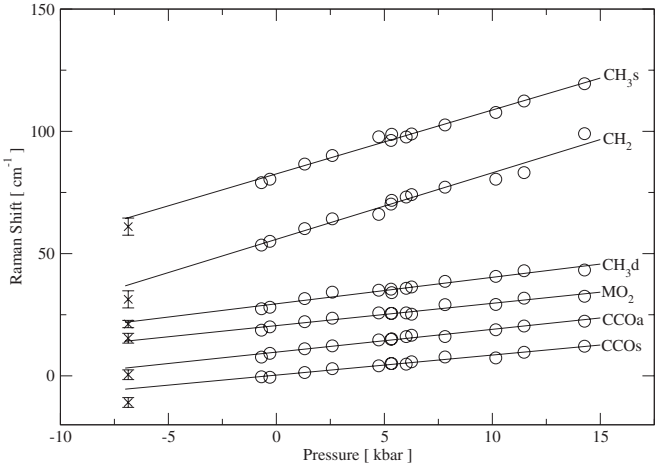

FIG. 4. The vibrational spectrum peak frequency shifts for various modes in ethanol as a function of uniform hydrostatic pressure as determined from molecular dynamics simulation. The ethanol vapor data are offset by the pressure equivalent of the cohesive energy density. Individual modes are offset vertically for clarity.

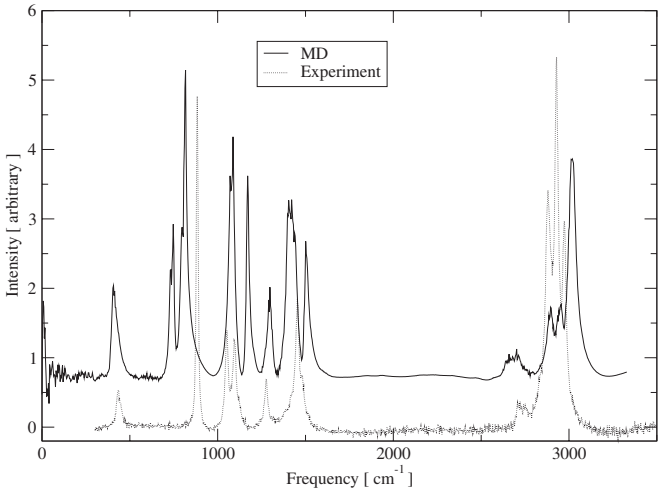

FIG. 3. The vibrational spectrum of ethanol obtained from molecular dynamics simulation by the Fourier transform of the autocorrelation function compared with the Raman spectrum from experiment (Ref. 4). The MD data are offset vertically by 0.75 units for clarity.

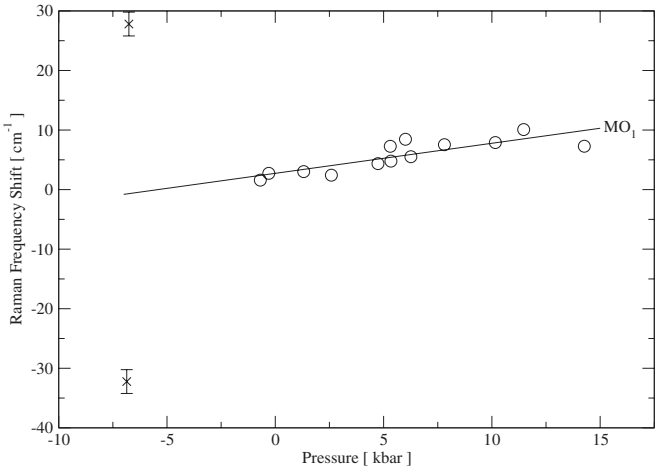

FIG. 5. The vibrational spectrum peak frequency shifts for the MO_1 mode in ethanol as a function of uniform hydrostatic pressure as determined from molecular dynamics simulation. The ethanol vapor data (representing two peaks) are offset by the pressure equivalent of the cohesive energy density.

IV. CONCLUSION

The results of explicit-atom molecular dynamics simulations of ethanol liquid and vapor are presented. The Cornell field is used for the explicit-atom potentials with the term describing the two-body intramolecular C-H bond modified to a Morse potential to improve the accuracy of the C-H vibrational frequencies. Very good agreement with experiment is obtained for density, compressibility, and CED of the ethanol liquid. The liquid is subjected to applied hydrostatic pressure in the range −1 to 15 kbar at room temperature and the vibrational frequency spectra are calculated. The peak frequency of seven vibrational modes was found to be accurate to within 100 cm^{-1} of their experimental positions and the change of frequency as a function of pressure is consistent with Raman data. The change in bond length with pressure supports the solvation pressure model for all bonds except for O-H due to hydrogen bonding. We find that the O-H bond is lengthened with applied pressure in agreement with many similar observations (for example Refs. 14, 24, and 25).

We conclude that the solvation pressure model is a useful, simple model that correctly describes the change in bond length and vibrational spectra from vapor to liquid and that the results support the idea that solutes experience an applied pressure equivalent to the cohesive energy density of the liquid. This ubiquitous pressure, however, is masked by certain interaction such as hydrogen bonding which provides a dominant effect, leading to different bond length behaviors. This leaves us cautious as to the general applicability to systems in which hydrogen bonding is dominant such as, obviously, solutes in aqueous environments.

ACKNOWLEDGMENT

P.J.B. acknowledges the support of Engineering and Physical Sciences Research Council (UK).

*d.faux@surrey.ac.uk

[1] J. R. Wood, M. D. Frogley, E. R. Meurs, A. D. Prins, T. Peijs, D. J. Dunstan, and H. D. Wagner, J. Phys. Chem. B **103**, 10388 (1999).
[2] J. R. Wood, M. D. Frogley, A. D. Prins, D. J. Dunstan, and H. D. Wagner, High Press. Res. **18**, 153 (2000).
[3] J. R. Wood, Qing Zhao, M. D. Frogley, E. R. Meurs, A. D. Prins, T. Peijs, D. J. Dunstan, and H. D. Wagner, Phys. Rev. B **62**, 7571 (2000).
[4] N. W. A. van Uden, H. Hubel, D. A. Faux, A. C. Tanczos, B. Howlin, and D. J. Dunstan, J. Phys.: Condens. Matter **15**, 1577 (2003).
[5] S. Dixit, W. C. K. Poon, and J. Crain, J. Phys.: Condens. Matter **12**, L323 (2000).
[6] N. W. A. van Uden, H. Hubel, D. A. Faux, D. J. Dunstan, and C. A. Royer, High Press. Res. **23**, 205 (2003).
[7] C. M. Dobson, Nature (London) **426**, 884 (2003).
[8] T. L. Religa, J. S. Markson, U. Mayor, S. M. V. Freund, and A. R. Fersht, Nature (London) **437**, 1053 (2005).
[9] M. Sadqi, D. Fushman, and V. Monuz, Nature (London) **442**, 317 (2006).
[10] Y. Ishibashi, T. Mishina, and J. Nakahara, Phys. Status Solidi B **243**, 1159 (2006).
[11] A. F. M. Barton, J. Chem. Educ. **48**, 156 (1971).
[12] A. F. M. Barton, *Handbook of Solubility Parameters and Other Cohesion Parameters*, 2nd ed. (CRC Press, Boca Raton, 1991).
[13] K. S. Schweizer and D. Chandler, J. Chem. Phys. **76**, 2296 (1982).
[14] M. R. Zakin and D. R. Herschbach, J. Chem. Phys. **89**, 2380 (1988).
[15] Y. Melendez-Pagan and D. Ben-Amotz, J. Phys. Chem. B **104**, 7858 (2000).
[16] W. D. Cornell, P. Cieplak, C. I. Bayly, I. R. Gould, K. M. Merz, D. M. Ferguson, D. C. Spellmeyer, T. Fox, J. W. Caldwell, and P. A. Kollman, J. Am. Chem. Soc. **117**, 5179 (1995).
[17] S. L. Mayo, B. D. Olafson, and W. A. Goddard, J. Phys. Chem. **94**, 8897 (1990).
[18] C. I. Bayly, P. Cieplak, W. D. Cornell, and P. A. Kollman, J. Phys. Chem. **97**, 10269 (1993).
[19] T. E. Cheatham, M. F. Crowley, T. Fox, and P. A. Kollman, Proc. Natl. Acad. Sci. U.S.A. **94**, 9626 (1997).
[20] M. P. Allen and D. J. Tildesley, *Computer Simulation of Liquids* (Oxford University Press, Oxford, 2002).
[21] D. M. Heyes, M. J. Cass, J. G. Powles, and W. A. B. Evans, J. Phys. Chem. B **111**, 1455 (2007).
[22] W. Smith and T. R. Forester, J. Mol. Graphics **14**, 136 (1996).
[23] *CRC Handbook of Chemistry and Physics*, 87th ed., edited by D. R. Lide (CRC Press, Boca Raton, FL, 2006).
[24] E. Fishman and H. G. Drickamer, J. Chem. Phys. **24**, 548 (1956).
[25] A. M. Benson and H. G. Drickamer, J. Chem. Phys. **27**, 1164 (1957).